Arabian Journal of Chemistry (2022) **15**, 104179

King Saud University

Arabian Journal of Chemistry

www.ksu.edu.sa
www.sciencedirect.com

ORIGINAL ARTICLE

Application of *Forsskaolea tenacissima* mediated gold nanoparticles in dyes discolouration, antibiotics removal, and metal ions detection

Wajheeba Khan [a], Nargis Jamila [a,*], Naeem Khan [b,*], Rehana Masood [c], Tan Wen Nee [d], Naheed Bibi [a], Joon Ho Hong [e], Amir Atlas [f]

[a] *Department of Chemistry, Shaheed Benazir Bhutto Women University, Peshawar 25000, Khyber Pakhtunkhwa, Pakistan*
[b] *Department of Chemistry, Kohat University of Science and Technology, Kohat 26000, Khyber Pakhtunkhwa, Pakistan*
[c] *Department of Biochemistry, Shaheed Benazir Bhutto Women University, Peshawar 25000, Khyber Pakhtunkhwa, Pakistan*
[d] *Chemistry Section, School of Distance Education, Universiti Sains Malaysia, 11800 Penang, Malaysia*
[e] *Nanobio Research Center, Jeonnam Bioindustry Foundation (JBF), Jangsung-gun, Jeollanam-do 57248, South Korea*
[f] *Institute of Basic Medical Sciences, Khyber Medical University, Peshawar 25000, Khyber Pakhtunkhwa, Pakistan*

Received 22 May 2022; accepted 7 August 2022
Available online 11 August 2022

KEYWORDS

Forsskaolea tenacissima;
AuNPs;
Dyes degradation;
Antibiotics removal;
Metal ions detection

Abstract Synthesis of nanoparticles using plant extract is environment-friendly, cost-effective, and sustainable. This study reports the synthesis of aqueous and ethanolic extracts mediated gold nanoparticles of aerial parts of *F. tenacissima* (FTAAuNPs) using chloroauric acid. The synthesized nanoparticles obtained from aqueous and ethanolic extracts under sunlight in 1:15 and 1:10 ratios with localized surface plasmon resonance (LSPR) peaks at 533 nm exhibited sizes of 15.7 nm and 27.6 nm, respectively, as revealed by scanning electron, transmission electron, and atomic force microscopic (SEM, TEM, AFM) techniques. Sharp intense surface plasmon resonance (SPR) peaks were obtained at basic pH (8 to 11), however, the same peaks broadened and reduced at elevated temperatures. FTAAuNPs demonstrated an efficient removal (> 80%) of dyes such as methylene blue (70%), Congo red (80%), methyl orange (82%), Rhodamine B (50%), *ortho*-nitrophenol (85%) and *para*-nitrophenols (85%), and antibiotics (amoxicillin, levofloxacin, doxycycline) up to 90%. Furthermore, FTAAuNPs were successfully used for sensing of Pb^{++}, Cu^{++}, Ni^{++}, and

* Corresponding authors.
E-mail addresses: nargisjamila@sbbwu.edu.pk, njk985@gmail.com (N. Jamila), naeem@kust.edu.pk, nkhan812@gmail.com (N. Khan).
Peer review under responsibility of King Saud University.

Production and hosting by Elsevier

https://doi.org/10.1016/j.arabjc.2022.104179

Zn^{++} ions in tap and river water samples. Hence, this study offers simple, cost effective, and efficient removal of pollutants/hazards in the water samples, and could solve water and sanitation problems especially in Pakistan.

1. Introduction

Nanotechnology deals with nanoscale materials of various shape and sizes (1–100 nm) and their applications. Among the huge variety of nanomaterials, metal nanoparticles (MNPs) have gained considerable attention in analytical, medical, biotechnology, electronics, and environmental remediation domains, due to their unique optical, electronic, and catalytic properties (Azharuddin et al. 2019; Mir et al. 2017; Ovais et al. 2018). Among the NPs, metal nanoparticles (MNPs) of gold (Au) and silver (Ag) are the most studied and easily synthesized nanomaterials, due to their remarkable optical, electrical and photothermal properties, facile synthesis, easily controllable size and shape, and good biocompatibility. In addition, high reactivity of these NPs, along with their unique binding affinity for certain molecules make them suitable for applications in sensing, diagnostics, labeling and antimicrobial activities (Khatoon et al. 2018).

Various physical, chemical and biological methods are employed for the synthesis of NPs. The chemical and physical techniques are toxic, expensive and also involve the use of extreme conditions which require huge energy consumption and hence are environment-unfriendly. On the other hand, the synthesis of NPs using biological sources such as plants, fungi, algae, and bacteria, is simple, inexpensive, safe and non-toxic. These biological sources contain biomolecules (phenolics, flavonoids, terpenoids, glycosides, and steroids), which act as reducing agents instead of the toxic chemicals used in other methods (Mondal et al. 2020; Saratale et al. 2018). NPs synthesized using synthetic reducing agents, are generally considered toxic. Therefore, NPs synthesis using plant parts; leaves, roots, flower, and seeds is the cleaner, nontoxic, and environmentally benign choice (Beyene et al. 2017; Omran et al. 2021). AuNPs as nanorods, nanowires, nanotubes, squares/rectangles, hexagons, and truncated triangles have been reported in literature as biosensors in diagnostics and therapy, and drug delivery. These applications of AuNPs are attributed to their favourable optical and physical properties, and surface area (Elahi et al. 2018; Zhang et al. 2020).

Discharge of effluents containing unfixed dyes, pharmaceuticals/antibiotics, and toxic metals including arsenic (As), lead (Pb), cadmium (Cd), and mercury (Hg) into water bodies from textile, paper, plastic, paint, printing, leather, pharmaceutical, and chemical industries is a serious threat to the environment (Saravanan et al. 2021). Synthetic organic unfixed dyes/colourants such as malachite green, Rhodamine B (RdB), methylene blue (MB), methyl orange (MO), and Congo red (CR) are released into soil and water, and considered hazardous to human health, ecosystem, aquatic biota, and microorganisms (Jadhav et al. 2019). Similarly, extensive researches have reported the release of antibiotics to the environment posing serious treats to human life (Chaturvedi et al. 2021). Hence, the toxic dyes and the antibiotics in environment need regular and careful monitoring. Heavy metals are other pollutants distributed widely in aqueous bed via several anthropogenic activities such as industrialization, mining, weathering, and other human activities. Among these, As, Pb, Cd, and Hg are reported to cause serious damage (Pan et al. 2018; Renu et al. 2021). Hence, to protect environment, and ultimately human health, it is essential to develop efficient and cost effective methods for the detection and removal of these pollutants/contaminants.

Heterogeneous catalysts, which play a key role in chemical industries, are getting much focus due to high selectivity and yield. Due to unique physico-chemical properties such as high specific surface area and energy, usage in small quantity, nanomaterials are gaining high attention as catalysts. These nanocatalysts enhance the selectivity of the reactions as it occurs at lower temperature, reduce the side products/reactions, higher recycling rates and recovery of energy consumption. Hence, these catalysts are of great interest in green chemistry, environmental remediation, development of renewable energy, and energy production from biomass (Hodges et al. 2018; Sharma et al. 2015; Zhu et al. 2019). In recent years, in the environmental remediation, green synthesized NPs have received greater attention due to their simplicity, efficiency, effectiveness, and eco-friendly nature (David & Moldovan, 2020; Nguyen et al. 2021; Wang et al. 2020). For example, triangular and spherical shaped AuNPs synthesized using *Pogostemon benghalensis* leaf extract have shown photocatalytic degradation of methylene blue (Paul et al. 2015). Baruah et al. (2018) reported *Alpinia nigra* mediated synthesis of AuNPs, which efficiently catalyzed the degradation of methyl orange and Rhodamine B up to ~ 83 and 88 %, following pseudo first order model. In addition, Umamaheshwari et al. (2018) reported an effective catalytic property of green synthesized AuNPs in Congo red and methyl orange degradation. Similarly, Kumari and Meena (2020) reported the degradation of bromophenol blue and methyl red dyes via AuNPs synthesized using *Lawsonia inermis*.

Forsskaolea tenacissima (Urticaceae family) distributed in the dry mountains of Khyber Agency, Pakistan, is a rich source of bioactive terpenoids, flavonoids, polyphenolics, tannins, volatile oils, and amides (Assaf et al. 2018, 2019). The present investigation aimed to synthesize gold nanoparticles (FTAAuNPs) using *Forsskaolea tenacissima* as a green source and evaluate its application in water treatment. The current research work further reports FTAAuNPs as colorimetric analytical assay for discolouration/reduction of dyes/nitrophenols, removal of antibiotics, and metal ions detection in tap and river water samples. The dyes and nitrophenols were consisted of methylene blue (MB), Congo red (CR), methyl orange (MO), Rhodamine B (RdB), *ortho*-nitrophenol (ONP), *para*-nitrophenol (PNP) whereas antibiotics and metal ions included amoxicillin (AMX), doxycycline (DXC), levofloxacin (LFX), orelox (ORX), lead (Pb^{++}), copper (Cu^{++}), nickel (Ni^{++}), iron (Fe^{+++}), potassium (K^{+}), sodium (Na^{+}), magnesium (Mg^{++}), palladium (Pd^{++}), stannous (Sn^{++}), and zinc (Zn^{++}).

2. Materials and methods

2.1. Sample collection

The herb *F. tenacissima* (Fig. 1) was collected from the mountains of Tirah (Khyber Agency, Khyber Pakhtunkhwa, Pakistan) in the year 2019. The subject herb was taxonomically identified in the Department of Botany, University of Peshawar (Pakistan). Before use, the sample was cleaned, shade dried at ambient temperature, powdered, and stored until further use. Samples of tap water were collected from Shaheed Benazir Bhutto Women University Campus, and used without any pretreatment. The river water samples were obtained from Kabul River (Khyber Pakhtunkhwa, Pakistan). To remove particulate matter, the river water was pretreated using a 0.22 μm syringe filter, and the supernatant (in triplicate) was collected and stored at 4 °C.

Fig. 1 *F. tenacissima* herb collected from Tirah (Khyber Agency), Khyber Pakhtunkhwa, Pakistan.

2.2. Chemicals, reagents and instrumentation

All the chemicals used in this study were purchased from Sigma-Aldrich and Merck (Germany). Chloroauric acid hydrated ($HAuCl4{\cdot\cdot}4H_2O$, 99.9% pure) was used for FTAAuNPs synthesis. Dyes and nitrophenols (*ortho*- and *para*-) used in catalytic activity evaluation of FTAAuNPs were CR (98% pure), MB (95% pure), RdB (99% pure), MO (97% pure), ONP (98% pure), and PNP (98% pure). Antibiotic standards selected for this study were AMX (98% pure), DXC (97% pure), LFX (98% pure), ORX (98% pure). Salts used in metals sensing were lead acetate (97% pure), copper chloride (99% pure), nickel chloride (98% pure), iron chloride (99% pure), zinc acetate (99% pure), potassium nitrate (99% pure), sodium sulphate (98% pure), magnesium sulphate (97% pure), stannous chloride (97% pure), and palladium chloride (99% pure). Aqueous extract and reagent solutions were prepared with ultrapure deionized water (resistivity 18.2 MΩ.cm) obtained from a Milli-Q apparatus (Millipore, Bedford, MA, USA). Freshly prepared aqua regia and deionized water was used for glassware cleaning. To obtain absorption spectra of the reaction mixture, a UV–1800 spectrophotometer (Shimadzu, Japan) was used. Functional groups involvement, and the size and surface topography of the FTAAuNPs was conducted via FT-IR spectrometer (Bruker) and field emission-scanning electron microscope (FE-SEM, S-4800, Hitachi, Japan). The operating procedures were accelerating voltage; 15 kV, magnification; x2.0 k, working distance; 7.7 mm, and high lens mode. The morphology of FTAAuNPs was observed under a transmission electron microscope, TEM (Phillips CM12, Eindhoven, Netherlands), operating at 120 kV. The samples were stained using uranyl acetate and placed on copper grid to be examined using TEM.

2.3. Synthesis of FTAAuNPs

Green synthesis of FTAAuNPs was performed using ultrapure water as well as natural ethanol as extracting solvents. For extracts preparation, a finely powdered material of *F. tenacissima* (5 g) in deionized water (50 mL) and natural ethanol (50 mL) as extracting solvents were separately extracted at 40–50 °C and 500 rpm for 2 h. The obtained extracts were filtered, and the final volume of the filtrate was adjusted to 100 mL by washing the vegetal residue with the respective solvents (deionized water and ethanol). Briefly, the obtained extracts were mixed with $HAuCl_4{\cdot}4H_2O$ salt solution in different ratios (extract: salt; 1:5, 1:7, 1:9, 1:10, and 1:15) and reacted under the conditions of stirring, heating, incubation (25–30 °C in dark), and sunlight at different intervals of time (0 min to 180 min/3h). The visual colour change from yellow to dark red/purple indicated production of AuNPs, which was later on confirmed by appearance of AuNPs specific SPR (surface plasmon resonance) band in UV–vis analysis. The reaction mixture of the synthesized AuNPs was centrifuged followed by washing with deionized water. The obtained product was stored in airtight vial until further use. In addition, effect of several factors such as pH (1 to 14, varied with buffer solutions) and temperature (30–80 °C) on FTAAuNPs (original pH 5.5–6.0) was investigated.

2.4. Discolouration/reduction of dyes/nitrophenols via FTAAuNPs

The catalytic activity of FTAAuNPs was measured for the discoloration of dyes including CR, MB, RdB and MO, and nitrophenols such as ONP and PNP in the presence of $NaBH_4$ (reducing agent) in an aqueous medium. The experiment was conducted following established published methods (Jamila et al. 2020; Khan et al. 2021). In this time-dependent experiment, briefly, 2.5 mL of 0.1 mM dyes/nitrophenols and 0.5 mL of 0.1 mM $NaBH_4$ were mixed in a UV–vis cuvette (1 cm path length). The UV–vis spectra were recorded from 200 to 800 nm regular time intervals for a period of 100 min. A similar experiment was conducted, in which a 5 mg of FTAAuNPs was added to the mixture of dyes/nitrophenols (2.5 mL) and $NaBH_4$ (0.5 mL) in a UV–vis cuvette, and the absorbance was recorded by UV–Vis spectrophotometer. The reduction of dyes was indicated by discoloration/decrease in the absorbance of dyes/nitrophenols' respective SPR bands, and calculated via equation (1) given below.

$$\%\text{decolourization/reduction} = (1 - \text{At/A0}) \times 100 \quad (1)$$

Where A_0 is the initial absorbance (absorbance of dyes at time "0″) and A_t is the absorbance of dyes at time "t".

Linear relationship and rate constant (k) was deduced from pseudo 1st order kinetics as shown in equation (2), where $[C_0]$ is the initial concentration of the dyes and $[C_t]$ is the concentration at time "t".

$$k = 1/t \ln [C0]/[Ct] \quad (2)$$

2.5. Removal of antibiotics from aqueous media by FTAAuNPs

For this assay, slightly modified published procedures of Wang et al. (2017) and Makropoulou et al. (2020) were followed.

Working solutions (0.001 to 0.1 mM) were prepared by dissolving the corresponding antibiotics in either water or absolute ethanol depending on the solubility. A series of experiments were conducted. First, only the UV spectra of antibiotics working solutions of 0.001 to 0.1 mM were recorded. Then, a quantity of FTAAuNPs (5 mg) with antibiotic solutions (2.5 mL) were mixed. The UV–vis spectra of these mixtures were measured at intervals of 0–180 min. To determine the removal percent (R%) of antibiotics, the following equation (3) was used in which C_0 and C represent the initial and final concentrations of the studied antibiotics, respectively.

$$R\% = (C0 - C)/C0 * 100 \quad (3)$$

In the final series of experiments, the practical application of FTAAuNPs in antibiotics removal was determined with two types of aqueous media (tap and river water samples). A 5 mg FTAAuNPs with antibiotic solutions (1.5 mL) and real water samples (1.5 mL) were mixed and the UV–vis spectra were measured at intervals of 0–180 min.

2.6. Metal ions detection in aqueous media via FTAAuNPs

Practical application of the synthesized FTAAuNPs was analyzed for Pb^{++}, Cu^{++}, Ni^{++}, Fe^{+++}, K^{+}, Na^{+}, Mg^{++}, Sn^{++}, Zn^{++}, and Pd^{++} ions recognition following published procedure (Anwar et al. 2018; Jamila et al. 2021). Briefly, the spiking of samples was carried out with the corresponding ion solutions (0.001–0.1 mM). The spiked samples (500 µL) were then added to a mixture of FTAAuNPs (500 µL) and water samples (500 µL). The resulting solutions were equilibrated at room temperature for 15 min and then the UV–vis spectra were recorded.

3. Results and discussion

3.1. Synthesis, spectral properties, and characterization of FTAAuNPs

For FTAAuNPs synthesis, an eco-friendly, rapid, and cost effective green method was adopted. In this synthesis, colourimetric/visible change of the reaction mixture in which a colloidal dispersion of AuNPs nanofluids lead to a color change from yellow to ruby red or bluish, was the preliminary evidence for AuNPs synthesis (Fig. S1, supplementary material). In the experimental procedure, FTAAuNPs synthesized in various ratios (1:5, 1:7, 1:9, 1:10; and 1:15) have shown that aqueous extract afforded significant AuNPs in 1:15 ratio whereas ethanolic extract significantly yielded AuNPs in 1:10 when reacted in sunlight. These NPs exhibited SPR absorption bands at 533 nm assigned to $\pi \rightarrow \pi^*$ and $n \rightarrow \pi^*$ transitions in the visible region (500–600 nm) (Fig. 2). From the results, it was found that with increasing reaction time (0 min to 180 min/3h), the SPR band gets intense, indicating reasonable FTAAuNPs production. The λ^{max} of SPR band depends on the size, shape, and concentration of AuNPs, solvent type, and the temperature of reaction mixture (Jang et al. 2022). The UV–vis spectra of AuNPs produced via aqueous extract contained one SPR peak whereas that of ethanolic extract included two peaks. According to Dzimitrowicz et al. (2019), the SPR peak at λ^{max} 520–550 nm is due the spherical nanostructures whereas the second SPR peak at λ^{max} 300–350 nm is attributed to aggregation or production of different shaped nanostructures. Other mixtures (1:5, 1:7, 1:9, 1:10, aqueous and ethanolic extracts) did not yield any reasonable FTAAuNPs (Figs. S2 and S3, supplementary material).

A pH and reaction temperature are the factors affecting synthesis, size, surface morphology, and stabilizing potential of the NPs. To optimize the conditions, FTAAuNPs were synthesized at different pH and temperatures. From the results (Fig. S4a, supplementary material), it has been deduced that pH affected the SPR intensity and λ^{max}. For example, at acidic pH, FTAAuNPs are destabilized and agglomerated as reported previously in several studies (Liu et al. 2010; Luo et al. 2019; Umamaheswari et al. 2018). In our study, as the solution becomes basic (pH 8 to 11), the sharp intense SPR peaks were obtained, which indicated the dispersed and stabilized FTAAuNPs. Examining the effect of temperature (30 °C, 40 °C, 50 °C, 60 °C, 70 °C, and 80 °C), from the results (Fig. S4b, supplementary material), it was observed that there is a small effect of increasing temperature on the broadening of SPR accompanied by reduced intensity and a slight bathochromic shift of λ^{max}. According to Link & El-Sayed (1999), to determine the significant effect on broadening, a temperature needs to be raised by several hundred degrees in order to record a significant line broadening. Overall, the optimum conditions where stable *F. tenacissima* mediated AuNPs can be produced might be a pH ranging from 8 to 12, and a temperature of 30 °C-50 °C.

The class of the phytoconstituents present in *F. tenacissima* extracts and functional groups involvement in NPs synthesis were determined via FT-IR spectroscopic method. In the FT-IR spectra of extracts (Fig. S5, supplementary material), the absorption bands at 3330 cm^{-1}, 2900 cm^{-1}, 1700–1600 cm^{-1} were attributed to the stretching vibration of –COOH, –NO, –NH, and –CH groups. Regarding the absorption frequencies of FTAAuNPs, absorption bands of –COOH, –NH, and C—H groups either were of reduced intensities or disappeared, which concludes the involvement of the subject groups in FTAAuNPs synthesis (Jamila et al. 2020; Liu et al. 2010; Luo et al. 2019; Umamaheswari et al. 2018).

In order to determine the size and shape of the produced FTAAuNPs, SEM, TEM, and AFM analyses were performed. Fig. 3 showing SEM, TEM, and AFM images, and particle size distribution graphs, depicts that aqueous and ethanolic extracts mediated FTAAuNPs possess an average size of 15.7 nm and 27.6 nm, respectively.

3.2. Discolouration/reduction of dyes/nitrophenols via FTAAuNPs

Based on high surface reactivity, large surface area, strong adsorption capacity, high catalytic efficiency, and simple analysis protocol, several colorimetric AuNPs sensors have been developed to detect pollutants such as dyes, antibiotics, and heavy metals (Saravanan et al. 2021). Organic dyes are synthetic chemical compounds released by several industries. The unfixed dyes are absorbed by soil and water, which may severely affect the environment/ecosystem, human health, and agricultural productivity (Jadhav et al. 2019). Hence, to control and manage the environmental remediation, recently, several researchers carried out investigation on the use of

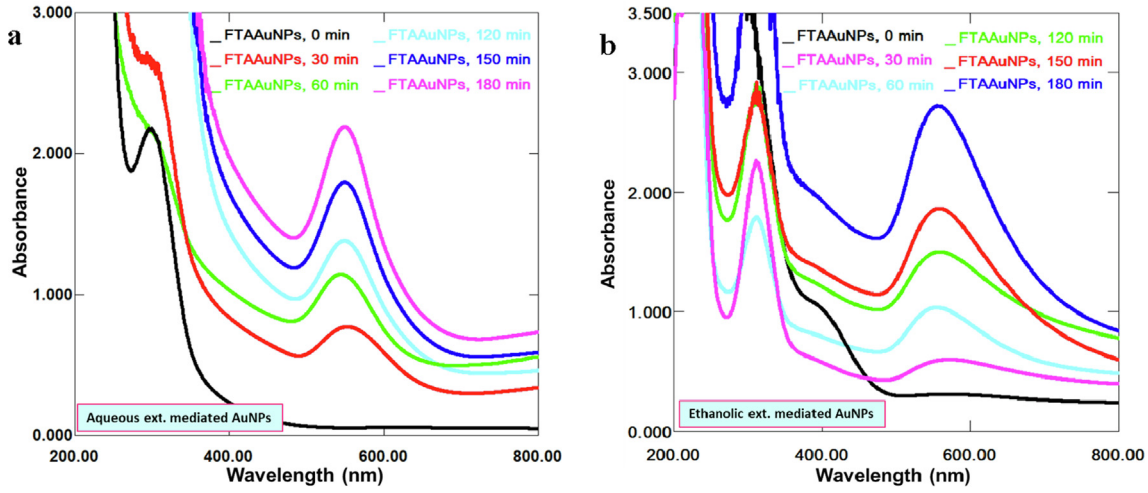

Fig. 2 Successive absorption spectra of FTAAuNPs using (a) aqueous extract (1:15) and (b) ethanol extract (1:10) reacted in sunlight.

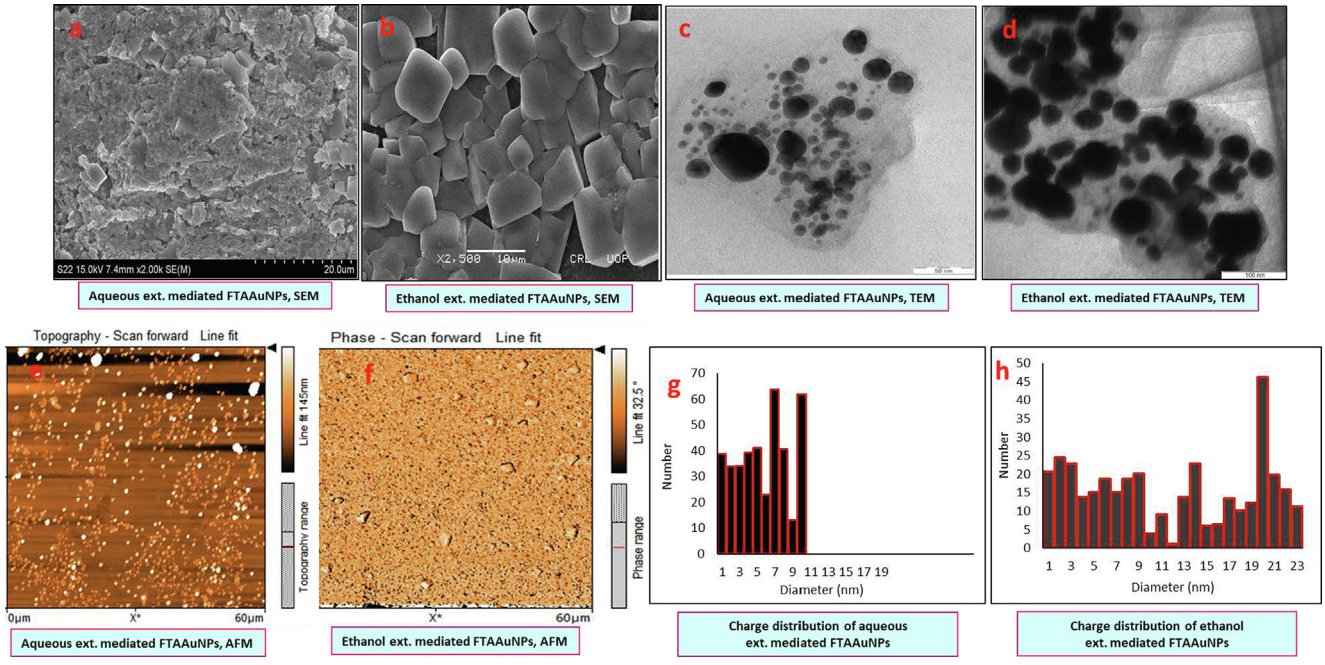

Fig. 3 Size and morphology by SEM (a, b), TEM (c, d), AFM (e, f) images, and particle size distribution graphs (g, h) of the aqueous and ethanol extracts synthesized FTAAuNPs, respectively.

NPs as efficient catalysts in the discolouration/reduction of dyes (David & Moldovan, 2020; Khan et al. 2021; Nguyen et al. 2021). The present study investigated and monitored the reduction/discolouration of dyes and nitrophenols including MB, CR, MO, RdB, ONP, and PNP in a time dependent manner. MB, which is a cationic dye exists as an oxidized (sharp blue colour) as well as reduced leucomethylene blue (colourless) form. The MB exhibits λ^{max} at 653 nm, 591 nm, and 290 nm due to $\pi \rightarrow \pi^*$ and $n \rightarrow \pi^*$ transitions, while its reduced form appears at 255 nm. By the addition of $NaBH_4$, dyes are reduced inefficiently, which is attributed to the large differences in the redox potential of the acceptor (dye) and donor (BH_4^- ions) (Cavuslar et al. 2020; Nadaf & Kanase, 2019). Hence, the reduction reaction by $NaBH_4$ is thermally allowed but kinetically forbidden, and it does not bring any significant change in dyes absorbance even in excess as indicated in previous reports (David & Moldovan, 2020; Jadhav et al. 2019; Jamila et al. 2020; Khan et al. 2021; Nguyen et al. 2021; Umamaheswari et al. 2018). However, when FTAAuNPs was added to the reaction mixture of MB, the absorbance at 653 and 290 nm declined with a simultaneous growth at 255 nm (Fig. 4a). This simultaneous decrease and increase in the absorbance indicated MB discolouration. Similarly, in case of CR, which shows λ^{max} at 487 and 349 nm due to $\pi \rightarrow \pi^*$ and $n \rightarrow \pi^*$ transitions (David & Moldovan, 2020; Jadhav et al. 2019; Khan et al. 2021; Nguyen et al. 2021; Umamaheswari et al. 2018), in the presence of FTAAuNPs, the absorbance decreased and the colour become faint due to

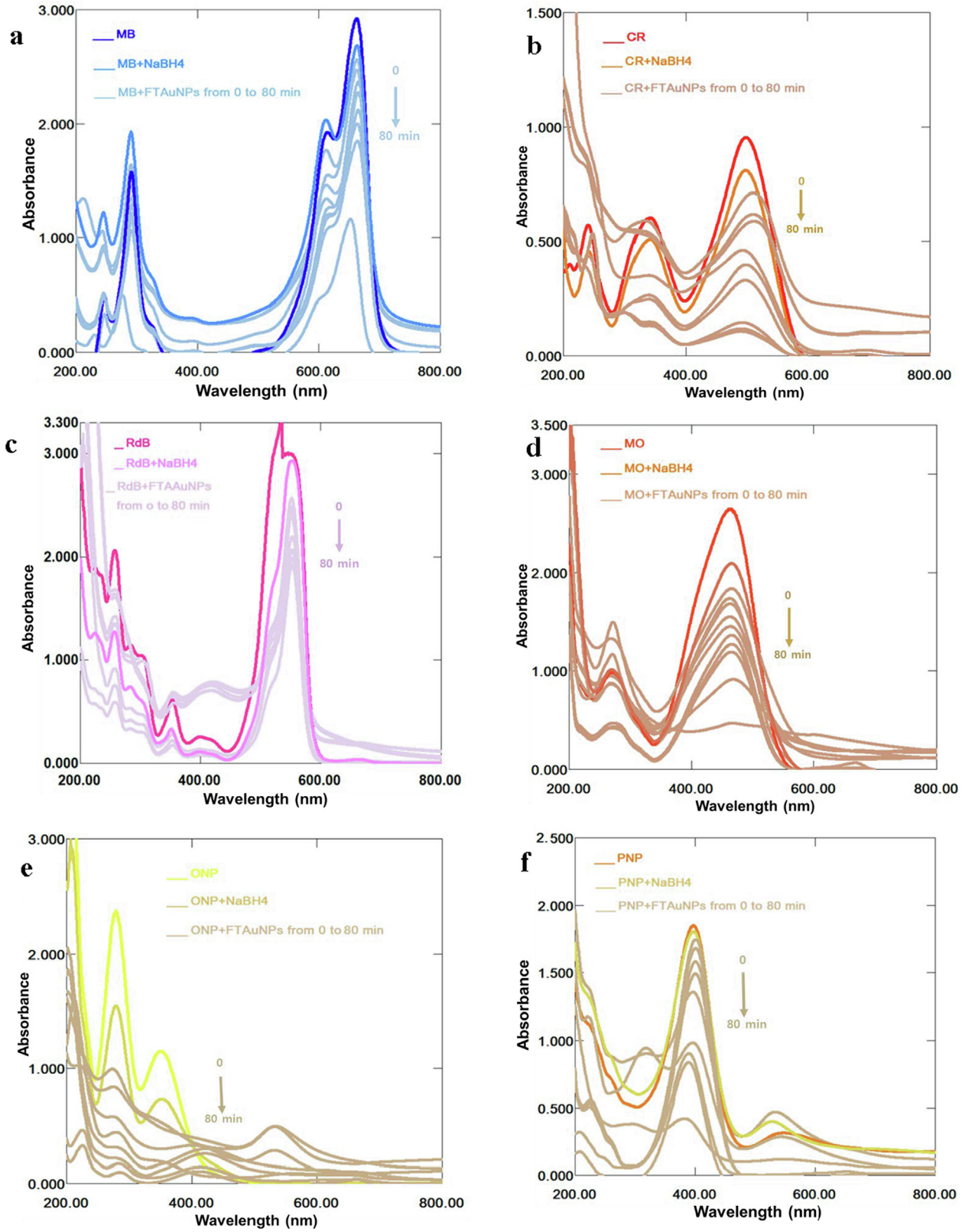

Fig. 4 Successive UV–Vis absorption spectra for the catalytic potential of FTAAuNPs at time interval of 0 (absorption maxima), 10, 20, 30, 40, 50, 60, 70, and 80 (absorption minima) min for (a) MB, (b) CR, (c) RdB, (d) MO, (e) ONP, (f) PNP, and (g) linear plots of $\ln(C/C_0)$ versus "t" in dyes/nitrophenols degradation/reduction process.

reduction process (Fig. 4b). Furthermore, for RdB, a cationic dye, which appears at 550 nm, the decrease in absorbance was recorded in a time-dependent absorbance spectrum on treating with FTAAuNPs (Fig. 4c). However, this decrease was insignificant and slow, which may be due to the weak adsorption of this dye on the surface of NPs. In case of MO, a decrease in intensity of λ^{max} at 462 nm and increase in absorption peak at 239 nm was observed (Fig. 4d). This increase of 239 nm is confined to amine group resulting from the MO degradation (Umamaheswari et al. 2018). From the results, it is clear that $NaBH_4$ alone does not efficiently discolourize dyes. However, in FTAAuNPs presence, the discolouration process significantly augmented. In addition, FTAAuNPs was also investigated for the reduction of *ortho-* and *para-*nitrophenols (Fig. 4e and f), which have shown high reduction rate for ONP followed by PNP. The rate of reaction of dyes and nitrophenols discoloration with FTAAuNPs was also calculated. From the results (Fig. 4g), it is revealed that the rate of reaction increases with increasing time, thus, the optimum discolouration of dyes (up to 90%) is achieved at 80 min, above which the reaction rate as well as the catalytic efficiency almost stopped. The dyes discolouration reactions followed pseudo first-order kinetics, where there is a linear correlation between "$\ln(C/C_0)$" and the corresponding reaction time, "t" (Fig. 4g). The values of pseudo first order rate constant (k) and the correlation coefficient (R^2) calculated using equation, $k = 1/t \ln [C_0]/[C_t]$ where $[C_0]$ and $[C_t]$ are the initial and the concentrations at a time "t", are listed in Table S1. The results obtained in the current study were consistent to several previous studies (Al-Ghamdi et al. 2022; Jadhav et al. 2019; Khan et al. 2021). The R^2 values obtained were from 0.9428 (RdB) to 0.9957 (ONP) showing that the dyes and nitrophenols discoloration/reduction fitted in the pseudo first order kinetics. The rate constant values indicated that ONP and CR degradation is faster than rest of the dyes followed by PNP, MO, and MB dyes, respectively, under similar experimental conditions.

Based on previous literature, the possible mechanism for the discolouration/reduction of dyes may be linked to redox reaction where FTAAuNPs act as electron donating species and dyes as electron accepting species. In the catalytic reduction, the BH_4^- molecules act as a nucleophile (electron donor) and generate the metal hydride by reacting with AuNPs surface, which further reacts with adsorbed (on AuNPs surface) azo groups due to electron relay between the $NaBH_4$ and azo groups of dyes. Thus, the degradation of azo dyes preliminary proceeded via hydrogenation of azo group (–N═N–) and then formation of the amine product ($–NH_2$) (Fu et al., 2019; Xiong et al. 2021). Furthermore, Khan et al. (2021) explained that the H^+ and OH^- generated in redox reaction reduces the chromophore of the dye, hence, decolorized the dyes molecule. In addition, according to Langmuir-Hinshelwood mechanism, the substrate (dyes/nitrophenols) and reductant ($NaBH_4$) both adsorbed on the surface of FTAAuNPs, which provided electrons to the substrate for their discoloration.

3.3. Removal of antibiotics from aqueous media by FTAAuNPs

The way of entering antibiotics into the environment is the effluents/wastewater released from pharmaceutical industries, hospitals, sewage treatment, and other aquatic media. The residual antibiotics released to the aqueous media can be harmful and toxic to ecosystem and human health. Therefore, their assessment and removal from the environment is very important. Depending on dispersibility, pH, temperature, and type, nature and volume of antibiotics, various types of antibiotics have different potential to adsorb on NPs, and hence, optimal removal may differ for different antibiotics (Chaturvedi et al. 2021; Makropoulou et al. 2020). In this study, removal of several antibiotics such as AMX, DXC, LFX, and ORX from water samples using FTAAuNPs were investigated. A series of experiments given in Fig. 5a-d determined the absorbance of different concentrations (0.001 to 0.1 mM) antibiotics solutions, and that of antibiotics solutions treated with FTAAuNPs. The results showed the decrease in the concentration/ absorbance of the mixtures of antibiotics solutions and FTAAuNPs. For AMX (Fig. 5a), which exhibits absorption peaks at the wavelengths 228 nm and 277 nm, FTAAuNPs needed 120–180 min to adsorb the subject antibiotics optimally with 80–95% efficiency. Similarly, λ^{max} (272 nm) for DXC (Fig. 5b) and LFX (288 nm) shown in Fig. 5c were decreased with increasing contact time (0 to 180 min). For ORX, the results are unclear and insignificant. The decrease in absorbance indicates the decrease in the concentration due to adsorption of antibiotics on the NPs surface, and ultimately removal of antibiotics from water samples as suggested by previous studies (Malakootian et al. 2019; Weng et al. 2018).

A parameter of pH could affect the electrostatic interaction between adsorbent and adsorbate. Hence, to optimize the antibiotics adsorption capacity on NPs, a pH is often taken into consideration. Most of the NPs contain carboxyl (COOH) and hydroxyl (OH) surface functional groups. Hence, upon interaction with antibiotics, an increase in pH results in the functional groups' protonation-deprotonation transition. At low pH, the protonation of functional groups of NPs cause them positively charged, whereas with the increase of pH, the gradual deprotonation of the functional groups takes place, making the surfaces negatively charged (Chaturvedi et al. 2021; Makropoulou et al. 2020; ul Ain et al. 2018;). Hence, with high pH ranges, the cationic antibiotic ions can be easily captured by NPs. Furthermore, the adsorption capacity of NPs is also associated with the characteristics of antibiotics. In our study, we found that increasing pH, the AMX and LFX capture was significantly affected whereas, for DXC and ORX, there was no clear effect on the adsorption (Fig. S6, supplementary material). Overall, except for ORX, an optimum removal (95 %) for the rest of the studied antibiotics was achieved. This competitive elimination of the antibiotic from water might be due to the nature of the antibiotic and the aqueous matrix (Makropoulou et al. 2020). From the kinetic modeling of the adsorption process, the removal of antibiotics by FTAAuNPs followed the pseudo-first order with the linear equations, R^2 and the rate constant values given in Table S1 (supplementary material). Experiments in aqueous media including tap water and river water were employed to test the practical performance of the removal of antibiotics in aqueous media. A series of known concentrations of antibiotics were added to the aqueous samples under the optimal experimental conditions, and the spectra were recorded. It was found that the antibiotics could be efficiently removed by FTAAuNPs (Fig. 5f-i).

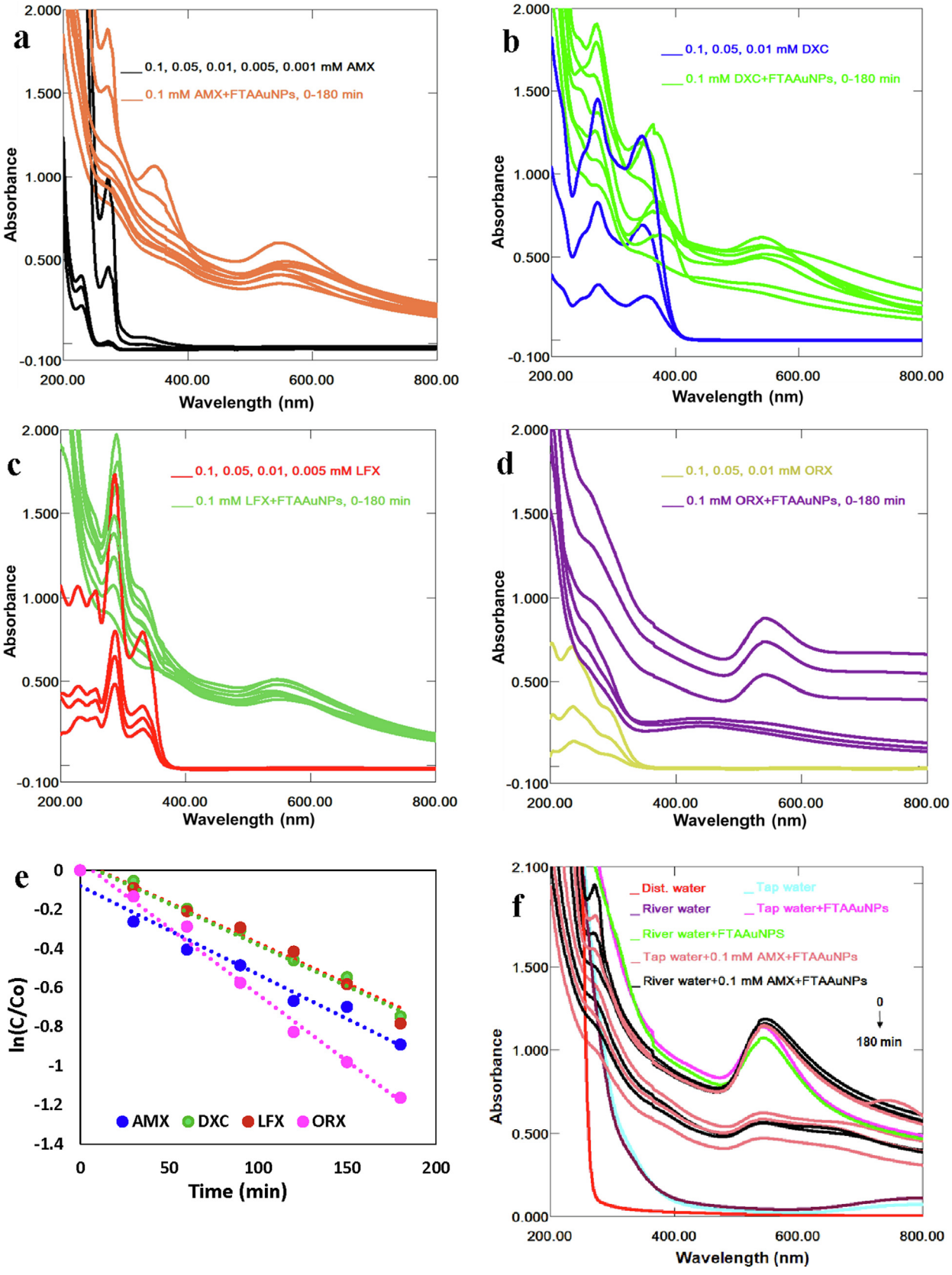

Fig. 5 Successive UV–Vis absorption spectra for antibiotics (a) AMX, (b) DXC, (c) LFX, (d) ORX, (e) linear plots of $\ln(C/C_0)$ versus "t", and (f) AMX (g) DXC, and (h) LFX, and (i) ORX removal from tap and river water samples by FTAAuNPs.

3.4. Metal ions detection in aqueous media via FTAAuNPs

The rapid and efficient technique for detecting heavy metal ions is the use of NPs, where the mechanism is based on observing color changes, and position and intensity of the SPR band of the mixture. These changes are due to the aggregation/agglomeration of NPs with the analyte (metal) through capping functional groups attached to the surface of AuNPs (Kim et al. 2017; Luo et al. 2019; Sang et al. 2018). In our study, the sensing ability of FTAAuNPs was evaluated with various metal ions such as Pb^{++}, Cu^{++}, Ni^{++}, Fe^{+++}, K^{+}, Na^{+}, Mg^{++}, Sn^{++}, Zn^{++}, and Pd^{++}. Adding metal ions to FTAAuNPs, there was no remarkable change in the position and intensity of SPR band, and the color of FTAAuNPs solution with Fe^{+++}, K^{+}, Na^{+}, Mg^{++}, Sn^{++}, and Pd^{++}. However, by the addition of Pb^{2+}, Cu^{++}, Ni^{++}, and Zn^{++} ion solutions to FTAAuNPs, the colour of the solutions changed from red to blue grey, which could be easily observed with naked eyes. Furthermore, a decrease and disappearance of SPR band (539 nm), and appearance of broad absorption peak above 700 nm of FTAAuNPs in the UV–vis spectra (Fig. 6) was observed, which corresponds to aggregation of FTAAuNPs as investigated by Deng et al. (2020) and Keskin et al. (2022). This indicates the subject metal ions detection, which might be due to induced destabilization and aggregation of FTAAuNPs by the ions. From the results, it was observed that the aggregation by Pb^{++} ions is stronger than Cu^{++}, Ni^{++}, and Zn^{++} ions. This aggregation might be due to the stronger chelating ability of Pb^{++} ions with hydroxyl and carboxyl groups on AuNPs surface, which induced destabilization of net negative charge on FTAAuNPs surface, consequently causing agglomeration of FTAAuNPs as reported earlier (Kim et al. 2017; Luo et al. 2019; Sang et al. 2018; Sheikh et al. 2021). Determining the effect of concentrations of metals ions, it was found that the intensity of the SPR band gradually reduced with increasing concentration of Pb^{++}, Cu^{++}, Ni^{++}, and Zn^{++} ion solutions. To evaluate the applicability of the proposed detection method, the developed probe was applied to determine the subject metal ions in the real water (tap and river water) samples. The results of UV–vis spectra demonstrated the broad and reduced intensity of SPR bands (Fig. 6), which confirmed the utility of the developed nanosensor for the accurate detection of Pb^{++}, Cu^{++}, Ni^{++}, and Zn^{++} ions in water sam-

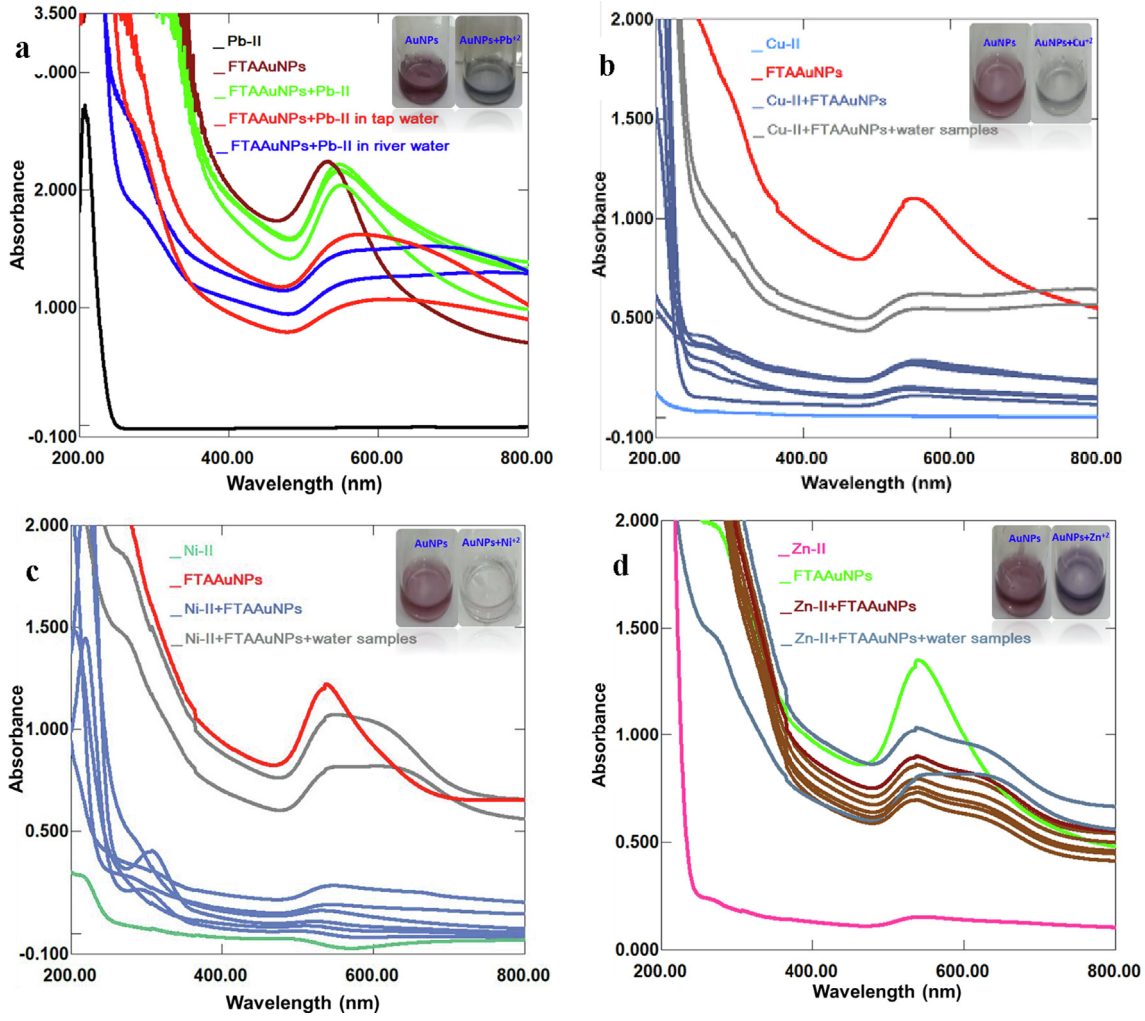

Fig. 6 Successive UV–Vis absorption spectra for sensing of metal ion solutions (a) Pb^{2+}, (b) Cu^{2+}, (c) Ni^{2+}, and (d) Zn^{2+} in tap and river water samples by FTAAuNPs.

ples. The other metals; Fe^{+++}, K^{+}, Na^{+}, Mg^{++}, Sn^{++}, and Pd^{++} did not exhibit any prominent change in color, as well as the position and intensity of SPR bands (Fig. S7, supplementary material).

Overall, from the current study, it was observed that the synthesized FTAAuNPs are helpful in significant degradation of ONP, CR, MO, and PNP to an 85%, whereas for MB and RdB, its catalytic efficiency is not reasonable. Furthermore, antibiotics removal up to 90% from water samples was obtained only for AMX, DXC, and LFX. In sensing several metal ions in water samples, the subject AuNPs were found effective and efficient only for Pb^{++}, Cu^{++}, Ni^{++}, and Zn^{++} ions.

4. Conclusions

This is the first study on eco-friendly green synthesis of AuNPs using *F. tenacissima* aqueous and ethanolic extracts with no additional chemical agents. The synthesized FTAAuNPs were applied in the discolouration of dyes/nitrophenols, removal of antibiotics, and probing metal ions in real water samples. FTAAuNPs successfully degraded/reduced MO (90%), CR (85%), ONP (85%), and PNP (85%) at intervals of 80 min. The subject FTAAuNPs were found helpful in removal of antibiotics including amoxicillin, doxycycline, and levofloxacin with 95% removal efficiency from aqueous media. Furthermore, in sensing metals in water samples, the subject AuNPs were found effective for some metals including Pb^{++}, Cu^{++}, Ni^{++}, and Zn^{2++} ions. The subject study reveals that FTAAuNPs is a new adsorbent for degradation/reduction of dyes/nitrophenols (CR, MO, ONP, and PNP), removal of antibiotics (AMX, DXC, LFX) from aqueous solution, and probing Pb^{++}, Cu^{++}, Ni^{++}, and Zn^{2++} ions in real water samples. Hence, to provide cleaner water, the subject FTAAuNPs could be used as a probe for water treatment and sanitation problems.

Declaration of Competing Interest

The authors declare that they have no known competing financial interests or personal relationships that could have appeared to influence the work reported in this paper.

Acknowledgement

This research study was supported by the research grants; 8967/KPK/NRPU/R&D/HEC/2017 and No.9_/R&D/SBBWURG/ORIC. The authors are thankful to the Higher Education Commission (HEC) and Shaheed Benazir Bhutto Women University Peshawar (SBBWUP) for awarding the projects.

Appendix A. Supplementary data

Supplementary data to this article can be found online at https://doi.org/10.1016/j.arabjc.2022.104179.

References

Al-Ghamdi, Y.O., Jabli, M., Soury, R., Khan, S.A., 2022. Synthesis of copper oxide nanoparticles using *Pergularia tomentosa* leaves and decolorization studies. Int. J. Phytoremediation 24, 118–130. https://doi.org/10.1080/15226514.2021.1926914.

Anwar, A., Minhaz, A., Khan, N.A., Kalantari, K., Afifi, A.B.M., Shah, M.R., 2018. Synthesis of gold nanoparticles stabilized by a pyrazinium thioacetate ligand: A new colorimetric nanosensor for detection of heavy metal Pd (II). Sens. Actuat. B. Chem. 257, 875–881. https://doi.org/10.1016/j.snb.2017.11.040.

Assaf, H.K., Nafady, A.M., Allam, A.E., Hamed, A.N., Kamel, M.S., Shimizu, K., 2018. Forsskamide, a new ceramide from aerial parts of *Forsskaolea tenacissima* Linn. Nat. Prod. Res. 32, 2452–2456. https://doi.org/10.1080/14786419.2017.1419234.

Assaf, H.K., Nafady, A.M., Allam, A.E., Hamed, A.N., Kamel, M.S., 2019. Promising antidiabetic and wound healing activities of *Forsskaolea tenacissima* L. aerial parts. J. Adv. Biomedical Pharm. Sci. 2, 72–76 https://dx.doi.org/10.21608/jabps.2019.7542.1034.

Azharuddin, M., Zhu, G.H., Das, D., Ozgur, E., Uzun, L., Turner, A. P., Patra, H.K., 2019. A repertoire of biomedical applications of noble metal nanoparticles. Chem. Commun. 55, 6964–6996. https://doi.org/10.1039/C9CC01741K.

Baruah, D., Goswami, M., Yadav, R.N.S., Yadav, A., Das, A.M., 2018. Biogenic synthesis of gold nanoparticles and their application in photocatalytic degradation of toxic dyes. J. Photochem. Photobiol. B. Biol. 186, 51–58. https://doi.org/10.1016/j.jphotobiol.2018.07.002.

Beyene, H.D., Werkneh, A.A., Bezabh, H.K., Ambaye, T.G., 2017. Synthesis paradigm and applications of silver nanoparticles (AgNPs), a review. Sustain. Mater. Technol. 13, 18–23. https://doi.org/10.1016/j.susmat.2017.08.001.

Cavuslar, O., Nakay, E., Kazakoglu, U., Abkenar, S.K., Ow-Yang, C. W., Acar, H.Y., 2020. Synthesis of stable gold nanoparticles using linear polyethyleneimines and catalysis of both anionic and cationic azo dye degradation. Mater. Adv. 1, 2407–2417. https://doi.org/10.1039/D0MA00404A.

Chaturvedi, P., Shukla, P., Giri, B.S., Chowdhary, P., Chandra, R., Gupta, P., Pandey, A., 2021. Prevalence and hazardous impact of pharmaceutical and personal care products and antibiotics in environment: A review on emerging contaminants. Environ. Res. 194,. https://doi.org/10.1016/j.envres.2020.110664 110664.

David, L., Moldovan, B., 2020. Green synthesis of biogenic silver nanoparticles for efficient catalytic removal of harmful organic dyes. Nanomaterials 10, 202. https://doi.org/10.3390/nano10020202.

Deng, H.H., Huang, K.Y., Fang, Q.H., Lv, Y.P., He, S.B., Peng, H.P., Xia, X.H., Chen, W., 2020. Schiff base and Lewis acid-base interaction-regulated aggregation/dispersion of gold nanoparticles for colorimetric recognition of rare-earth Sc3+ ions. Sens. Actuat. B. Chem. 311,. https://doi.org/10.1016/j.snb.2020.127925 127925.

Dzimitrowicz, A., Berent, S., Motyka, A., Jamroz, P., Kurcbach, K., Sledz, W., Pohl, P., 2019. Comparison of the characteristics of gold nanoparticles synthesized using aqueous plant extracts and natural plant essential oils of *Eucalyptus globulus* and *Rosmarinus officenalis*. Arab. J. Chem. 12, 4795–4805. https://doi.org/10.1016/j.arabjc.2016.09.007.

Elahi, N., Kamali, M., Baghersad, M.H., 2018. Recent biomedical applications of gold nanoparticles: A review. Talanta 184, 537–556. https://doi.org/10.1016/j.talanta.2018.02.088.

Fu, Y., Qin, L., Huang, D., Zeng, G., Lai, C., Li, B., He, J., Yi, H., Zhang, M., Cheng, M., Wen, X., 2019. Chitosan functionalized activated coke for Au nanoparticles anchoring: Green synthesis and catalytic activities in hydrogenation of nitrophenols and azo dyes. Appl. Catal. B. Environ. 255,. https://doi.org/10.1016/j.apcatb.2019.05.042 117740.

Hodges, B.C., Cates, E.L., Kim, J.H., 2018. Challenges and prospects of advanced oxidation water treatment processes using catalytic nanomaterials. Nat. Nanotechnol. 13, 642–650. https://doi.org/10.1038/s41565-018-0216-x.

Jadhav, S.A., Garud, H.B., Patil, A.H., Patil, G.D., Patil, C.R., Dongale, T.D., Patil, P.S., 2019. Recent advancements in silica nanoparticles based technologies for removal of dyes from water. Colloids Interface Sci. Commun. 30,. https://doi.org/10.1016/j.colcom.2019.100181 100181.

Jamila, N., Khan, N., Bibi, A., Haider, A., Khan, S.N., Atlas, A., Nishan, U., Minhaz, A., Javed, F., Bibi, A., 2020. *Piper longum* catkin extract mediated synthesis of Ag, Cu, and Ni nanoparticles and their applications as biological and environmental remediation agen-ts. Arab. J. Chem. 13 (6425), 6436. https://doi.org/10.1016/j.arabjc.2020.06.001.

Jamila, N., Khan, N., Bibi, N., Waqas, M., Khan, S.N., Atlas, A., Amin, F., Khan, F., Saba, M., 2021. Hg (II) sensing, catalytic, antioxidant, antimicrobial, and anticancer potential of *Garcinia mangostana* and α–mangostin mediated silver nanoparticles. Chemosphere 272,. https://doi.org/10.1016/j.chemosphere.2021.129794 129794.

Jang, W., Yun, J., Eyimegwu, P.N., Hou, J., Byun, H., Kim, J.H., 2022. Controlling the formation of encapsulated gold nanoparticles for highly reactive catalysts in the homocoupling of phenylboronic acid. Catal. Today. 388–389, 109–116. https://doi.org/10.1016/j.cattod.2020.09.028.

Keskin, B., Üzer, A., Apak, R., 2022. Ionic liquid-modified gold nanoparticle-based colorimetric sensor for perchlorate detection via anion− π interaction. ACS Omega. (published online). https://doi.org/10.1021/acsomega.2c02078.

Khan, S.A., Bakhsh, E.M., Asiri, A.M., Khan, S.B., 2021. Synthesis of zero-valent Au nanoparticles on chitosan coated NiAl layered double hydroxide microspheres for the discoloration of dyes in aqueous medium. Spectrochim. Acta A. 250,. https://doi.org/10.1016/j.saa.2020.119370 119370.

Khatoon, U.T., Rao, G.N., Mohan, M.K., Ramanaviciene, A., Ramanavicius, A., 2018. Comparative study of antifungal activity of silver and gold nanoparticles synthesized by facile chemical approach. J. Environ. Chem. Eng. 6, 5837–5844. https://doi.org/10.1016/j.jece.2018.08.009.

Kim, D.Y., Shinde, S., Ghodake, G., 2017. Colorimetric detection of magnesium (II) ions using tryptophan functionalized gold nanoparticles. Sci. Rep. 7, 1–9. https://doi.org/10.1038/s41598-017-04359-4.

Kumari, P., Meena, A., 2020. Green synthesis of gold nanoparticles from *Lawsonia inermis* and its catalytic activities following the Langmuir-Hinshelwood mechanism. Colloids Surf. A: Physicochem. Eng. Asp. 606,. https://doi.org/10.1016/j.colsurfa.2020.125447 125447.

Link, S., El-Sayed, M.A., 1999. Size and temperature dependence of the plasmon absorption of colloidal gold nanoparticles. J. Phys. Chem. 103, 4212–4217. https://doi.org/10.1021/jp984796o.

Liu, Z., Zu, Y., Fu, Y., Meng, R., Guo, S., Xing, Z., Tan, S., 2010. Hydrothermal synthesis of histidine-functionalized single-crystalline gold nanoparticles and their pH–dependent UV absorption characteristic. Colloids Surf. B. 76, 311–316. https://doi.org/10.1016/j.colsurfb.2009.11.010.

Luo, X., Xie, X., Meng, Y., Sun, T., Ding, J., Zhou, W., 2019. Ligands dissociation induced gold nanoparticles aggregation for colorimetric Al^{3+} detection. Anal. Chim. Acta 1087, 76–85. https://doi.org/10.1016/j.aca.2019.08.045.

Makropoulou, T., Kortidis, I., Davididou, K., Motaung, D.E., Chatzisymeon, E., 2020. Photocatalytic facile ZnO nanostructures for the elimination of the antibiotic sulfamethoxazole in water. J. Water Process Eng. 36,. https://doi.org/10.1016/j.jwpe.2020.101299 101299.

Malakootian, M., Yaseri, M., Faraji, M., 2019. Removal of antibiotics from aqueous solutions by nanoparticles: a systematic review and meta analysis. Environ. Sci. Pollut. Res. 26, 8444–8458. https://doi.org/10.1007/s11356-019-04227-w.

Mir, M., Ahmed, N., Rehman, A.U., 2017. Recent applications of PLGA based nanostructures in drug delivery. Colloids Surf. B. 159, 217–231. https://doi.org/10.1016/j.colsurfb.2017.07.038.

Mondal, P., Anweshan, A., Purkait, M.K., 2020. Green synthesis and environmental application of iron–based nanomaterials and nanocomposite: A review. Chemosphere 127509. https://doi.org/10.1016/j.chemosphere.2020.127509.

Nadaf, N.Y., Kanase, S.S., 2019. Biosynthesis of gold nanoparticles by *Bacillus marisflavi* and its potential in catalytic dye degradation. Arab. J. Chem. 12, 4806–4814. https://doi.org/10.1016/j.arabjc.2016.09.020.

Nguyen, D.T.C., Le, H.T., Nguyen, T.T., Nguyen, T.T.T., Bach, L.G., Nguyen, T.D., Tran, V.T., 2021. Multifunctional ZnO nanoparticles bio-fabricated from *Canna indica* L. flowers for seed germination, adsorption, and photocatalytic degradation of organic dyes. J. Hazard. Mater., 126586 https://doi.org/10.1016/j.jhazmat.2021.126586.

Omran, B.A., Whitehead, K.A., Baek, K.H., 2021. One-pot bioinspired synthesis of fluorescent metal chalcogenide and carbon quantum dots: Applications and potential biotoxicity. Colloids Surf. B 200,. https://doi.org/10.1016/j.colsurfb.2021.111578 111578.

Ovais, M., Zia, N., Ahmad, I., Khalil, A.T., Raza, A., Ayaz, M., Sadiq, A., Ullah, F., Shinwari, Z.K., 2018. Phyto-therapeutic and nanomedicinal approaches to cure Alzheimer's disease: present status and future opportunities. Front. Aging Neurosci. 10, 284. https://doi.org/10.3389/fnagi.2018.00284.

Pan, S., Lin, L., Zeng, F., Zhang, J., Dong, G., Yang, B., Jing, Y., Chen, S., Zhang, G., Yu, Z., Sheng, G., Ma, H., 2018. Effects of lead, cadmium, arsenic, and mercury co-exposure on children's intelligence quotient in an industrialized area of southern China. Environ. Pollut. 235, 47–54. https://doi.org/10.1016/j.envpol.2017.12.044.

Paul, B., Bhuyan, B., Purkayastha, D.D., Dey, M., Dhar, S.S., 2015. Green synthesis of gold nanoparticles using *Pogestemon benghalensis* (B) O. Ktz. leaf extract and studies of their photocatalytic activity in degradation of methylene blue. Mater. Lett. 148, 37–40. https://doi.org/10.1016/j.matlet.2015.02.054.

Renu, K., Chakraborty, R., Myakala, H., Koti, R., Famurewa, A.C., Madhyastha, H., Vellingiri, B., George, A., Gopalakrishnan, A.V., 2021. Molecular mechanism of heavy metals (lead, chromium, arsenic, mercury, nickel and cadmium)-induced hepatotoxicity–A review. Chemosphere 271,. https://doi.org/10.1016/j.chemosphere.2021.129735 129735.

Sang, F., Li, X., Zhang, Z., Liu, J., Chen, G., 2018. Recyclable colorimetric sensor of Cr^{3+} and Pb^{2+} ions simultaneously using a zwitterionic amino acid modified gold nanoparticles. Spectrochim. Acta A 193, 109–116. https://doi.org/10.1016/j.saa.2017.11.048.

Saratale, R.G., Karuppusamy, I., Saratale, G.D., Pugazhendhi, A., Kumar, G., Park, Y., Hgodake, G.S., Bharagava, R.N., Banu, R., Shin, H.S., 2018. A comprehensive review on green nanomaterials using biological systems: Recent perception and their future applications. Colloids Surf. B 170, 20–35. https://doi.org/10.1016/j.colsurfb.2018.05.045.

Saravanan, A., Kumar, P.S., Jeevanantham, S., Karishma, S., Tajsabreen, B., Yaashikaa, P.R., Reshma, B., 2021. Effective water/wastewater treatment methodologies for toxic pollutants removal: Processes and applications towards sustainable development. Chemosphere 130595. https://doi.org/10.1016/j.chemosphere.2021.130595.

Sharma, N., Ojha, H., Bharadwaj, A., Pathak, D.P., Sharma, R.K., 2015. Preparation and catalytic applications of nanomaterials: a review. RSC Adv. 5, 53381–53403. https://doi.org/10.1039/C5RA06778B.

Sheikh, Z., Amin, M., Khan, N., Khan, M.N., Sami, S.K., Khan, S.B., Hafeez, I., Khan, S.A., Bakhsh, E.M., Cheng, C.K., 2021. Potential application of *Allium cepa* seeds as a novel biosorbent for efficient biosorption of heavy metals ions from aqueous solution. Chemosphere. 279,. https://doi.org/10.1016/j.chemosphere.2021.130545 130545.

ul Ain, N., Anis, I., Ahmed, F., Shah, M.R., Parveen, S., Faizi, S., Ahmed, S., 2018. Colorimetric detection of amoxicillin based on quercetagetin coated silver nanoparticles. Sens. Actuators B. 265, 617–624. https://doi.org/10.1016/j.snb.2018.03.079.

Umamaheswari, C., Lakshmanan, A., Nagarajan, N.S., 2018. Green synthesis, characterization and catalytic degradation studies of gold nanoparticles against congo red and methyl orange. J. Photochem. Photobiol. B 178, 33–39. https://doi.org/10.1016/j.jphotobiol.2017.10.017.

Wang, Z., Du, Y., Yang, C., Liu, X., Zhang, J., Li, E., Zhang, Q., Wang, X., 2017. Occurrence and ecological hazard assessment of selected antibiotics in the surface waters in and around Lake Honghu. China. Sci. Total Environ. 609, 1423–1432. https://doi.org/10.1016/j.scitotenv.2017.08.009.

Wang, L., Peng, X., Fu, H., Huang, C., Li, Y., Liu, Z., 2020. Recent advances in the development of electrochemical aptasensors for detection of heavy metals in food. Biosens. Bioelectron. 147,. https://doi.org/10.1016/j.bios.2019.111777 111777.

Weng, X., Cai, W., Lan, R., Sun, Q., Chen, Z., 2018. Simultaneous removal of amoxicillin, ampicillin and penicillin by clay supported Fe/Ni bimetallic nanoparticles. Environ. Pollut. 236, 562–569. https://doi.org/10.1016/j.envpol.2018.01.100.

Xiong, Y., Wan, H., Islam, M., Wang, W., Xie, L., Lü, S., Fijul Kabir, S.M., Liu, H., Mahmud, S., 2021. Hyaluronate macromolecules assist bioreduction (AuIII to Au0) and stabilization of catalytically active gold nanoparticles for azo contaminated wastewater treatment. Environ. Technol. Innov. 24,. https://doi.org/10.1016/j.eti.2021.102053 102053.

Zhang, J., Mou, L., Jiang, X., 2020. Surface chemistry of gold nanoparticles for health–related applications. Chem. Sci. 11, 923–936. https://doi.org/10.1039/C9SC06497D.

Zhu, W., Chen, Z., Pan, Y., Dai, R., Wu, Y., Zhuang, Z., Wang, D., Peng, Q., Chen, C., Li, Y., 2019. Functionalization of hollow nanomaterials for catalytic applications: nanoreactor construction. Adv. Mater. 31, 1800426. https://doi.org/10.1002/adma.201800426.